OPEN ACCESS Freely available online

PLoS PATHOGENS

Fz2 and Cdc42 Mediate Melanization and Actin Polymerization but Are Dispensable for *Plasmodium* Killing in the Mosquito Midgut

Shin-Hong Shiao[☯¤], Miranda M. A. Whitten[☯], Daniel Zachary, Jules A. Hoffmann, Elena A. Levashina[*]

Institut de Biologie Moléculaire et Cellulaire, UPR9022 du CNRS, Équipe ''Avenir'' INSERM, Strasbourg, France

The midgut epithelium of the mosquito malaria vector *Anopheles* is a hostile environment for *Plasmodium,* with most parasites succumbing to host defenses. This study addresses morphological and ultrastructural features associated with *Plasmodium berghei* ookinete invasion in *Anopheles gambiae* midguts to define the sites and possible mechanisms of parasite killing. We show by transmission electron microscopy and immunofluorescence that the majority of ookinetes are killed in the extracellular space. Dead or dying ookinetes are surrounded by a polymerized actin zone formed within the basal cytoplasm of adjacent host epithelial cells. In refractory strain mosquitoes, we found that formation of this zone is strongly linked to prophenoloxidase activation leading to melanization. Furthermore, we identify two factors controlling both phenomena: the transmembrane receptor frizzled-2 and the guanosine triphosphate–binding protein cell division cycle 42. However, the disruption of actin polymerization and melanization by double-stranded RNA inhibition did not affect ookinete survival. Our results separate the mechanisms of parasite killing from subsequent reactions manifested by actin polymerization and prophenoloxidase activation in the *A. gambiae–P. berghei* model. These latter processes are reminiscent of wound healing in other organisms, and we propose that they represent a form of wound-healing response directed towards a moribund ookinete, which is perceived as damaged tissue.

Citation: Shiao SH, Whitten MMA, Zachary D, Hoffmann JA, Levashina EA (2006) Fz2 and Cdc42 mediate melanization and actin polymerization but are dispensable for *Plasmodium* killing in the mosquito midgut. PLoS Pathog 2(12): e133. doi:10.1371/journal.ppat.0020133

Introduction

Few infectious diseases carry heavier economic and social burdens than malaria. Within *Anopheles* mosquitoes, the only natural vectors of human malaria, immune responses to the *Plasmodium* parasite are highly species and strain specific. However, two universal bottlenecks stand out: parasites suffer very heavy losses as they traverse the epithelia of the midgut and as they journey from the midgut to the salivary glands. The attrition of ookinetes in the mosquito midgut can therefore serve as an excellent model for the study of host–parasite interactions.

The *Plasmodium* sporogonic cycle is initiated when gametocytes are ingested by the mosquito during a blood meal. Gametocytes swiftly give rise to gametes, which fertilize in the midgut lumen. The zygotes thus formed develop into motile, banana-shaped ookinetes, which invade and traverse the midgut epithelium approximately 24 h after blood ingestion (depending on the host–parasite species combination). During this trip the majority of ookinetes are destroyed by host responses even in susceptible mosquito strains, but a few surviving ookinetes reach the basal side of the midgut and transform into oocysts, which mature over the next 10–12 d to release thousands of sporozoites into the mosquito hemocoel. Sporozoites then journey through the hemolymph (blood) and invade the salivary glands. Successful salivary gland sporozoites are finally transmitted to a new vertebrate host via an infective bite.

In general terms, mosquitoes are able to mount efficient cell-mediated and humoral immune responses, and are equipped with an array of antimicrobial molecules, coagulation factors, opsonins, and recognition factors (for reviews, see [1,2]). Although the mechanisms of anti-*Plasmodium* defense are still poorly understood, the characterization of the *Anopheles gambiae* genome [3] has provided powerful new tools for functional analysis. Recent research has highlighted a role for a complement-related thioester-containing protein 1 (TEP1) in ookinete lysis and subsequent melanization [4]. However, the exact mode of TEP1-mediated killing is yet to be determined and probably involves further downstream factors. An additional molecule shown to be induced by *Plasmodium* infection is leucine-rich repeat immune protein 1 [5], whose silencing leads to a phenotype similar to that of TEP1. Depletion of the hemolymph-derived C-type lectin 4

Editor: Kasturi Haldar, Northwestern University Medical School, United States of America

Received August 3, 2006; **Accepted** November 6, 2006; **Published** December 29, 2006

Abbreviations: AZ, organelle-free actin zone; Cdc42, cell division cycle 42; dpi, days post-infection; dsRNA, double-stranded RNA; Fz2, frizzled-2; GFP, green fluorescent protein; hpi, hours post-infection; PPO, prophenoloxidase; SRPN, serine protease inhibitor; RNAi, RNA interference; TEM, transmission electron microscopy; TEP1, thioester-containing protein 1

* To whom correspondence should be addressed. E-mail: e.levashina@ibmc.u-strasbg.fr

☯ These authors contributed equally to this work.

¤ Current address: Department of Entomology, University of California Riverside, Riverside, California, United States of America

Synopsis

A dangerous journey awaits malaria *Plasmodium* parasites ingested by a mosquito. Most parasites are destroyed by host responses in the midgut, and in parasite-resistant refractory strains of mosquito the mortality can reach 100%. This midgut "bottleneck" represents an appealing target for reducing malaria transmission by the genetic control of wild mosquitoes. However, the killing mechanisms are still unclear. In this study, electron microscopical analyses followed the entire midgut invasion process in mosquitoes to identify the major site(s) and ultrastructural features of *Plasmodium* killing. The authors found that invasion can be divided into two steps: a swift passage through a midgut cell, followed by establishment of the parasite in the basal extracellular space, where it becomes an important target for destruction by soluble immunity factors. In refractory mosquitoes, dead parasites are associated with the formation of organelle-free zones of actin in adjacent midgut cells, and melanin deposition on the parasite surface. The authors identify two genes, called *frizzled-2* and *cell division cycle 42,* that control these phenomena. Actin zone formation and melanization are generally thought to be killing mechanisms; however, the authors show by gene silencing that neither is lethal to *Plasmodium*. Instead, these mechanisms may represent a form of mosquito wound-healing response that is triggered by the presence of a moribund parasite.

and of serine protease inhibitor (SRPN) 2 provokes spontaneous melanization of ookinetes [5] in non-melanizing mosquito strains. This suggests that these molecules control the early stages of prophenoloxidase (PPO) activation, which leads to ookinete melanization [6,7].

Genetic variability within a single mosquito species leads to substantial differences in individuals' permissiveness towards malaria parasites, and this has allowed laboratory selection and study of highly refractory mosquito strains (discussed by [8,9]). From *A. gambiae,* the most important malaria vector of sub-Saharan Africa, the L3–5 refractory strain has been selected. In this strain, ookinete development is completely terminated and accompanied by subsequent melanization of the parasite [10]. The parental G3 strain, from which L3–5 was derived, is considered "susceptible" since approximately 20% of invading ookinetes survive to the oocyst stage in the absence of melanization. Knockdown of *TEP1* or *leucine-rich repeat immune protein 1* by double-stranded RNA (dsRNA) completely abolishes melanotic refractoriness in the refractory L3–5 strain [4,5] and leads to hyper-parasitization in the susceptible G3 strain. All of the above immune factors are soluble and secreted by the hemocytes (blood cells) in the hemocoel, and as there is no direct contact between the hemocytes and the ookinetes, these factors have to pass through the midgut basal lamina to interact with the parasites located in the basal labyrinth [4] (reviewed by [11]).

Anti-*Plasmodium* responses may also be mediated by midgut factors. SRPN6 is produced by midgut epithelial cells in response to malaria infection [12]. The dsRNA knockdown of *SRPN6* results in a complex phenotype: it temporarily slows down ookinete killing in L3–5 mosquitoes, whilst simultaneously enhancing melanization [12]. Furthermore, the transcriptional responses of the *A. gambiae* midgut epithelium to *Plasmodium berghei* infection involve extensive regulation of genes controlling actin and microtubule cytoskeleton remodeling, of which some appear to modestly impair ookinete survival [13].

Early studies have reported organelle-free cellular zones formed by midgut epithelial cells at their point of contact with invading ookinetes. This event was first described by Vernick et al. [14] in *P. gallinaceum* infections of a refractory *A. gambiae* strain, and has very occasionally been seen in a fully susceptible strain, Fam5. Vernick et al. observed a finely fibrillar zone protruding from the epithelial cell basal labyrinth that encircled dead ookinetes. These organelle-free, actin-rich cytoplasmic formations, for which we propose the term "organelle-free actin zone" (AZ), have since been noted by other authors investigating different host–parasite species combinations (e.g., the "purse-string" [15,16]; the "lamellipodial hood" or "collar" [17]; and the "actin cone" or "ring" [18]). AZ-like structures are generally assumed to be involved in parasite killing or a consequence of an intracellular parasite exiting a damaged midgut cell, but a functional role in parasite killing has not been formally demonstrated.

We are interested in determining the predominant mode of ookinete killing in the *A. gambiae–P. berghei* infection model, and in redressing a paucity of electron microscope studies in this host–parasite species combination. Here, we aim to identify the precise location of dead ookinetes and to estimate the relative numbers of ookinetes that die in each compartment. In so doing, we hope to establish whether parasites are killed via exposure to soluble hemocyte-derived immunity factors in the extracellular milieu, or by midgut cell-mediated killing responses, or a combination of both. There is also a very clear need to resolve the functional significance of the AZ in terms of ookinete killing and its relationship with melanization. To address these points, we have used transmission electron microscopy (TEM) and confocal immunofluorescence microscopy in combination with RNA interference (RNAi)–dependent gene silencing, and have investigated AZ/ookinete co-localization, the composition of the AZ, its control by TEP1 or proteins involved in cytoskeletal rearrangement, and its potential role in parasite killing.

We show that the majority of ookinetes are killed by lysis in the extracellular space, rather than succumbing to intracellular killing. Moreover, in the refractory strain, we noted that the majority of dead and dying ookinetes were surrounded by melanin and a zone of polymerized actin within the adjacent midgut cells (the AZ). We show that both features are linked and dependent on TEP1 activity. We identified two genes controlling actin polymerization and melanization, *frizzled-2 (Fz2)* and *cell division cycle 42 (Cdc42)*. Silencing of both genes by RNAi did not affect parasite survival, demonstrating that AZ formation and melanization do not constitute the ookinete killing mechanism. Actin polymerization and PPO activation are both processes reminiscent of wound healing in other organisms (e.g., [19,20]). We propose that *Plasmodium* infection induces a wound-healing response in *A. gambiae,* which includes actin polymerization and PPO activation. However, these responses do not account for major parasite losses during invasion of the midgut.

Results

Ookinete Killing Is Predominantly Extracellular

Two major mechanisms have been described to account for ookinete killing in the mosquito midgut epithelium: the first involves destruction of intracellular parasites in apoptotic

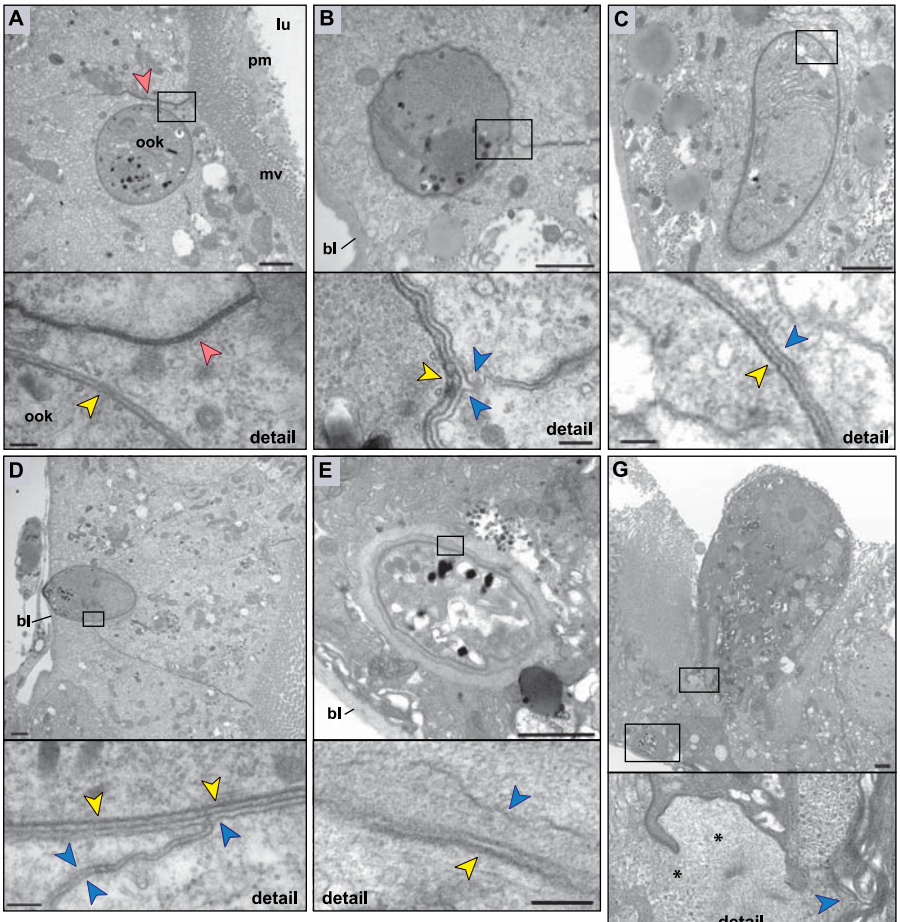

F

LOCATION in MIDGUT	OOKINETES observed	
	G3 (susceptible)	L3-5 (refractory)
In lumen, near microvilli	13	3
Intracellular: apical (near jc)	12 (8)	0 (0)
Intracellular: basal	3	0
Intercellular	32	21
Extracellular	77	59
TOTAL	**137**	**93**

Figure 1. TEM Images of *P. berghei* Ookinete Invasion of the *A. gambiae* Midgut

(A) Transient intracellular stage. An ookinete invades the apical (luminal) side of a susceptible G3 strain mosquito midgut cell. Note the proximity to the microvilli and cell junction (red arrow). Detail (box): intracellularity is confirmed by the absence of a host midgut cell membrane enclosing the ookinete double membrane (yellow arrow).

(B and C) Intercellular ookinetes in G3 (B) and L3–5 (refractory) (C) mosquito midguts. The parasites are now closer to the basal side of the gut. High magnification shows a triple membrane arrangement—that is, the ookinete double pellicle membrane (yellow arrow) is surrounded by the midgut cell membrane (blue arrow), indicating the parasite is outside the host cell.

(D and E) Ookinetes reaching the basal labyrinth and lamina are extracellular in both G3 (D) and L3–5 mosquitoes (E). Note that the adjacent midgut cells appear healthy. Arrows as in (B and C).

(F) Distribution of ookinetes in the midguts of G3 and L3–5 mosquitoes, as observed by TEM according to the criteria mentioned above. One hundred thirty-seven individual ookinetes were observed in G3 at regular intervals between 18 and 33 hpi, and 93 parasites were observed in L3–5 midguts. In both cases the majority of ookinetes were observed to be extracellular and only a small minority were intracellular. Most intracellular ookinetes were located apically, close to a cell junctional complex.

(G) An extracellular ookinete positioned below an apoptotic host cell (top). Fibrillar cytoplasmic regions (asterisks in first detail box) extend from the healthy adjacent cells towards the apoptotic cell and ookinete. Note the extensive membrane ruffling (blue arrow in first detail box) and the triple membrane arrangement surrounding an extracellular parasite (second detail box).

bl, basal lamina; jc, junctional complex; lu, midgut lumen; mv, microvilli; ook, ookinete; pm, peritrophic matrix.

Scale bars = 1 μm in main pictures and 0.1 μm in detail boxes.

doi:10.1371/journal.ppat.0020133.g001

cells of the infected midgut (the "time bomb" model [15,16,21–25]); in the second, ookinetes are proposed to be lysed in intercellular or extracellular spaces by soluble factors secreted from hemocytes [4,5]. To gain a better understanding of the killing mechanism in the *A. gambiae–P. berghei* model, we first identified the compartments occupied by parasites during traversal of the epithelium, and most importantly the location(s) in which ookinetes are killed. We examined ultra-thin midgut sections by TEM from both susceptible (G3) and refractory (L3–5) mosquito strains between 18 and 48 hours post-infection (hpi). An important overall observation was that the great majority (at least 80%)

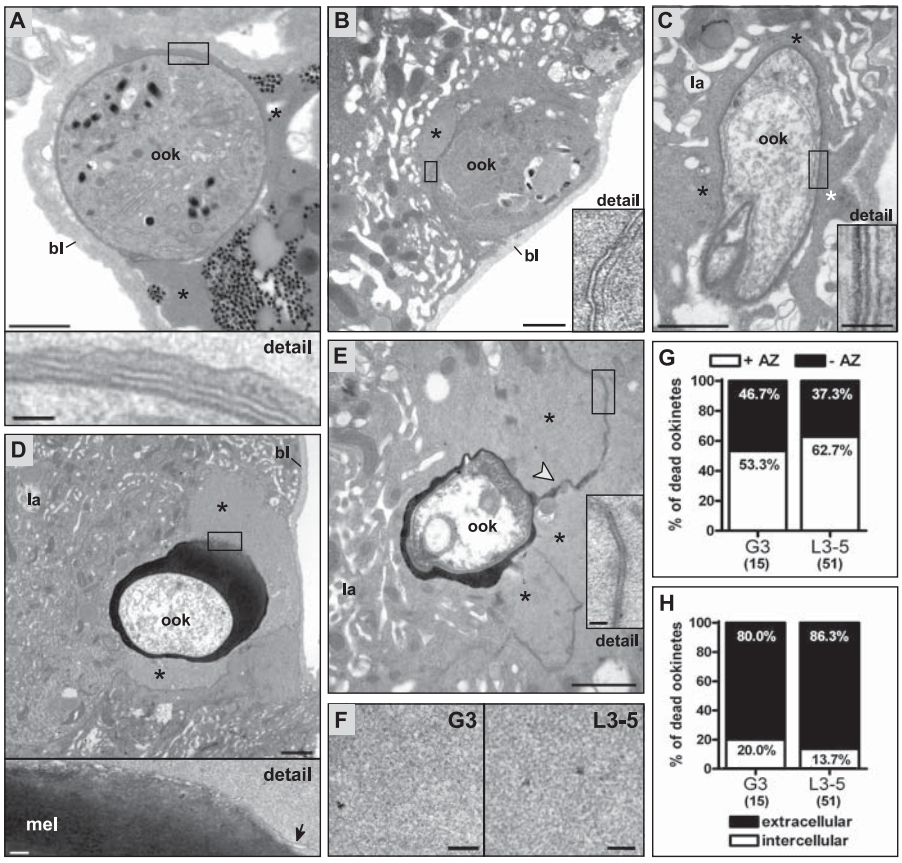

Figure 2. A Filamentous AZ Surrounds Extracellular Ookinetes

(A and B) A thin AZ (asterisks) forms from the cytoplasm of midgut cells to partially cover an ookinete in a susceptible (G3) mosquito. The ookinete is apparently healthy. Boxes: detail of the ookinete/midgut cell border showing the triple membrane indicative of an extracellular parasite. Note the proximity of the parasite to the basal lamina.

(C) A lysed ookinete in a susceptible mosquito surrounded by a thin AZ (asterisk). The parasite is extracellular (inset), and the membranes remain intact even though the organelles of the ookinete appear lysed.

(D) In refractory (L3–5) mosquitoes, a thicker AZ forms around dead or dying ookinetes, but not live parasites. The AZ is associated with melanin deposition. Melanization occurs in the extracellular space between the parasite and the midgut cell membrane (black arrow in detail box) and is thicker on the basal side closest to the hemocoel. Note that the midgut cells on either side of the ookinete are alive.

(E) A second melanized, dead ookinete associated with a thick AZ. The putative intercellular path of invasion is indicated by a trail of melanin that reacted with shed ookinete proteins (white arrowhead).

(F) High magnification of AZs from refractory and susceptible mosquitoes showing identical ultrastructural features. The zone is characterized by finely granular or filamentous material and is devoid of organelles (scale bar = 200 nm).

(G) The percentage of dead ookinetes associated with an AZ is higher in L3–5 mosquitoes than in the G3 strain.

(H) In both strains, the vast majority of dead parasites visible by TEM were extracellular and none appeared to be intracellular.

bl, basal lamina; la, basal labyrinth; mel, melanin; ook, ookinete; *, AZ.

Scale bars = 1 μm in main pictures and 0.1 μm in detail boxes, unless stated otherwise.

doi:10.1371/journal.ppat.0020133.g002

of ookinetes, particularly dead ones, were located outside the midgut epithelial cells in the intercellular or extracellular spaces of the epithelium at the level of the basal labyrinth (Figures 1 and 2).

The major features of successful ookinete invasions are represented in Figure 1, and were very similar between susceptible and refractory insects. Ookinete invasion of the midgut epithelium occurred between 18 and 33 hpi and involved a complex route, beginning at the apical (microvillous) surface and ending at the membranous labyrinth beneath the basal lamina (hemocoel side) where the oocyst developed. Ookinetes were found in intra-, inter-, and extracellular locations within the midgut epithelium (not necessarily representing consecutive steps), but predominantly in the extracellular compartment. We observed that in this infection system, the invasion of the midgut was often complete before full polymerization of the peritrophic matrix. Of note, peritrophic matrix development is significantly retarded at the relatively low temperature (20.5 °C) necessary for *P. berghei* development [26].

Only 11% of the ookinetes in susceptible mosquitoes (15 out of 137) and none (out of 93) in refractory mosquitoes were judged to be intracellular (Figure 1F), indicating either that this phase is extremely transient or that only a minority of ookinetes invade the cytoplasm of midgut cells. Intracellular parasites are characterized by the absence of the midgut epithelial membrane covering the double parasite pellicle membrane (Figure 1A), signifying that ookinetes are in direct contact with the cytoplasm of the epithelial cells. Approximately 80% of the intracellular ookinetes observed were located near the apical side of the invaded midgut cell, usually just beneath the microvilli and close to the junctional complex

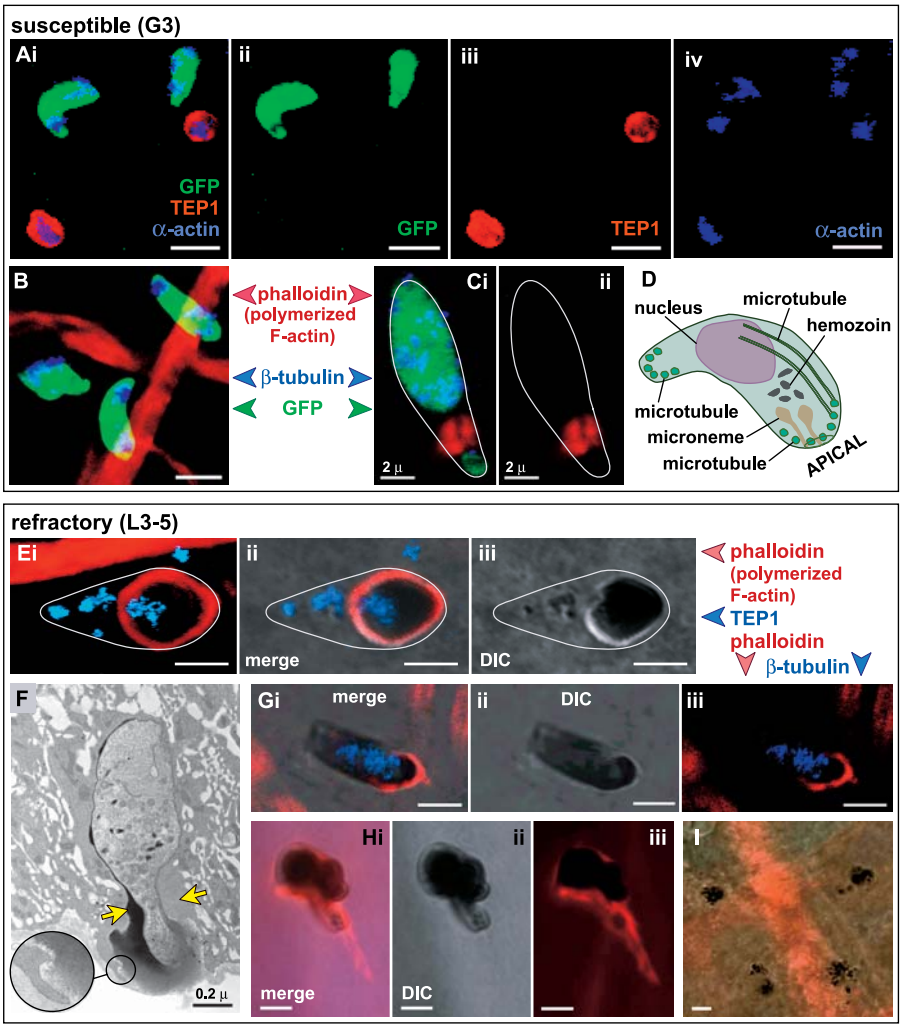

Figure 3. Biochemical Composition and Characteristics of the AZ

Confocal sections and 3-D reconstructions of *P. berghei*-infected midgut tissues.

(A–D) Ookinetes in susceptible (G3) mosquitoes, fixed at 28 hpi and showing ookinetes without associated AZs (A and B) and with AZs (C). (A) Non-polymerized (globular) α-actin is detected on both live (GFP-expressing) and dead ookinetes (stained in red for the killing factor TEP1). (B) Red phalloidin dye labels polymerized actin and heavily stains midgut muscle tissue. Live (GFP) parasites are stained blue with monoclonal antibody against β-tubulin. (C) A rare example of an AZ associated with a live (GFP) ookinete in a susceptible mosquito. The AZ is labeled red with phalloidin and does not co-localize with the blue β-tubulin signal, nor does its distribution pattern follow that of α-actin (A). The shape of the ookinete is indicated by a white outline. Note the parasite shape constriction at the AZ. (D) Cartoon of a typical ookinete indicating the arrangement of major cytoskeletal elements and organelles.

(E–I) Dead ookinetes in refractory (L3–5) mosquitoes, fixed at 28 hpi. DIC, differential interface contrast. (E) A red polymerized actin "halo" forms around a melanized ookinete that is stained in blue for the TEP1 killing factor. The ookinete shape is outlined in white. Note that the intensity of melanization is not uniform across the parasite but is concentrated at the same (basal) end as the halo. This concentration effect is seen more clearly by TEM ([F], yellow arrows), suggesting that the AZ can block melanin dispersal, which remains extracellular (see circle, bottom left). (G) The blue β-tubulin signal on a melanized ookinete does not co-localize with the red phalloidin-stained polymerized actin of the AZ (muscles are also phalloidin stained). (H) AZs containing polymerized actin form a range of shapes but do not uniformly cover the entire parasite, which may also display a range of shape constrictions. A long phalloidin-stained trail is seen behind this ookinete. Patterns of phalloidin staining are also affected by the viewing angle. (I) Dead ookinetes that are non-melanized are not covered by an AZ. Surrounding muscle is stained red with phalloidin, but the parasites (identified by dense clusters of hemozoin) remain unstained.

Scale bars = 5 μm unless otherwise stated.

doi:10.1371/journal.ppat.0020133.g003

(Figure 1A and 1F), suggesting that intracellular parasites represent ookinetes at the earliest stages of penetration of the midgut epithelium. The time-points of midgut dissections were sufficiently early to detect intracellular phases of invasion, because ookinetes were still observed in the midgut lumen approaching the microvilli (Figure 1F).

The vast majority of ookinetes in both mosquito strains were observed to be outside the midgut cells, but in extremely intimate contact with the midgut cell membranes (Figure 1C–1E), based on the observation of several sections. A triple membranous layer surrounding the ookinete is indicative of an inter- or extracellular location—that is, the outer membrane is contributed by the host midgut cell, and the inner two compose the pellicle membrane complex of the parasite. Importantly, *P. berghei* ookinetes were extracellular (55.5% in G3 and 71% in L3–5) or intercellular (23% in G3

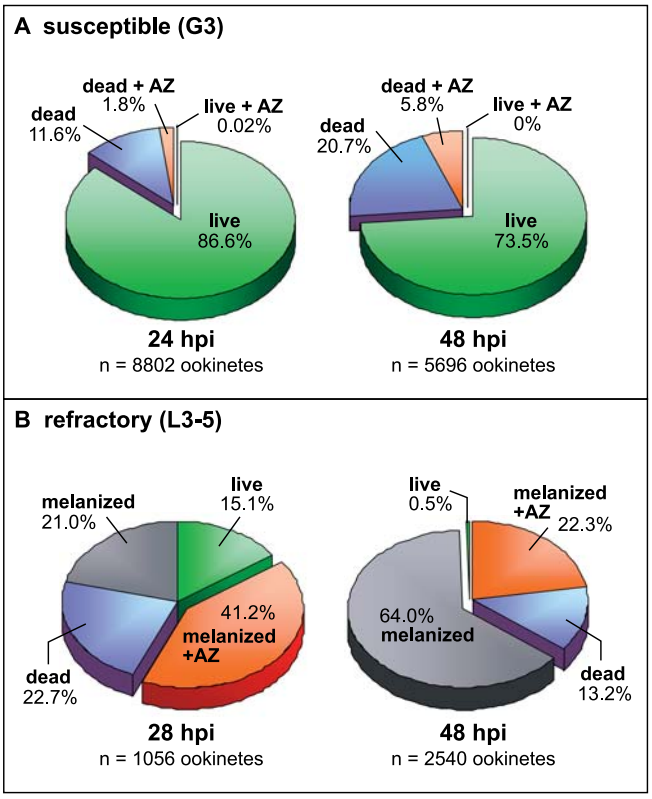

Figure 4. Different Fates of Ookinetes Infecting Refractory and Susceptible Mosquitoes, Determined by Phalloidin Staining

The majority of ookinetes in G3 (susceptible) mosquitoes (A) were alive at 24 and 48 hpi, and few ookinetes were surrounded by the AZ. In contrast, almost complete ookinete mortality in L3–5 (refractory) midguts (B) was associated with high levels of melanization and AZ formation. Note that the AZ exclusively surrounded melanized parasites in L3–5 guts. "Dead" refers to ookinetes that were fully lysed but not melanized or associated with an AZ.

doi:10.1371/journal.ppat.0020133.g004

and 25% in L3–5) during the time of peak parasite death (24–33 hpi) [4].

Apoptotic and necrotic cells were occasionally observed in both uninfected (not shown) and infected (Figure 1G) midguts, and healthy adjacent midgut cells extended filamentous cytoplasmic regions towards the dying cells. These extensions were organelle free and resembled the crawling lamellipodia or actin aggregates (described by [17,18]) that have been implicated in repair of the midgut epithelium. These zones often exhibited extensive membrane ruffling. Intercellular and extracellular ookinetes were sometimes found near extruding apoptotic midgut cells (e.g., Figure 1G), which did not appear to contain intracellular ookinetes. These observations suggest that the time bomb mechanism is not the predominant mode of *P. berghei* killing in *A. gambiae*.

In contrast to the projections associated with apoptotic midgut cells, we frequently observed additional filamentous zones surrounding lysed and dying ookinetes. Therefore, subsequent analyses were focused on the features of these zones.

A Filamentous AZ Surrounds Extracellular Ookinetes

A striking feature of ookinete presence in the basal extracellular midgut space is the appearance of a finely granular or filamentous, membrane-surrounded zone that forms as an extension of midgut cells immediately adjacent to dead or dying ookinetes (Figure 2A–2F).

This zone, which we call the AZ, is an organelle-free region of the midgut epithelial cell cytoplasm and is contained within its plasma membrane. We observed the AZ at the basal side of both susceptible (G3) and refractory (L3–5) *A. gambiae* midguts infected with *P. berghei,* and noted that the zones originated from healthy looking cells. The fine structure of the AZ was identical in L3–5 and G3 mosquitoes (Figure 2F). However, there were important differences between the strains in terms of zone thickness, frequency, and association with dead ookinetes. Few ookinetes in G3 mosquitoes displayed an AZ, and when they did, the AZ was usually thin (<200 nm) and surrounded both live (Figure 2A and 2B) and dead, lysed (Figure 2C) ookinetes. However, melanization did not occur. In contrast, AZs were more frequently observed in L3–5 mosquito midguts, and formed exclusively around dead or dying ookinetes (Figure 2D and 2E). The zones were normally much thicker (>500 nm) and always associated with melanization in this strain. Approximately 63% of all dead ookinetes within L3–5 midguts were surrounded by an AZ, compared with 53% of the dead parasites in G3 midguts, as judged by TEM (Figure 2G). Additionally, all of the dead ookinetes visible in our TEM study occurred in the extracellular or intercellular spaces (Figure 2H). Where a parasite contacted several cells, they all contributed to the AZ (e.g., Figure 2E).

The AZ and intracellular ookinetes did not co-localize in our study. We found that the AZ occurs only in the most basal region of the midgut, where the parasite is almost invariably extracellular. The triple membrane arrangement around the parasite (including both the apical and basal regions of the ookinete) indicated that the AZ did not form as a parasite exited a damaged midgut cell, but rather surrounded an extracellular parasite. The AZ did not usually cover the entire ookinete surface, and its extent and location on the ookinete surface varied (see Figures 2 and 3).

The AZ Is Composed of Polymerized Actin

To investigate the composition of the AZ, which is formed by healthy midgut cells, we used confocal and fluorescence microscopy with antibodies and specific dyes that discriminate between various cytoskeletal proteins. The AZ was not stained by an antibody raised against non-polymerized or globular forms of α-actin, nor by anti-β-tubulin. Both antibodies nevertheless recognized ookinete proteins at sites corresponding to microtubule and cytoskeleton assembly (Figure 3). However, polymerized or filamentous actin, as detected by the dye phalloidin, specifically stained the AZ (and midgut muscle fibers) in L3–5 and G3 mosquitoes, and did not stain the parasites. In G3 mosquitoes, the phalloidin staining of the thin AZ was often much fainter than in the L3–5 strain.

Phalloidin-stained collar- or halo-shaped zones on melanized (dead) ookinetes in the L3–5 mosquitoes are shown in Figure 3E, 3G, and 3H. These images also demonstrate that the AZ is often associated with shape constrictions of the parasite and can limit the dispersal of melanin pigment so that it appears concentrated at one end of the parasite (Figure 3E and 3F). Ookinetes are known to be melanized first at their apical tips closest to the basal lamina, reflecting the

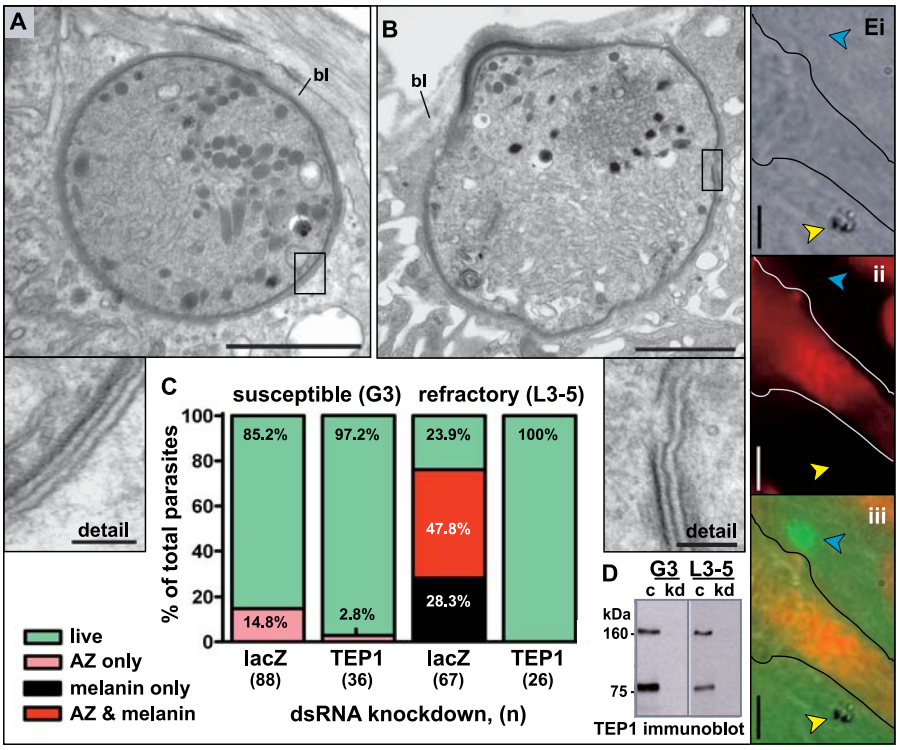

Figure 5. The AZ and Melanization Are Depleted by *TEP1* RNAi

(A and B) dsRNA-mediated knockdown of *TEP1* expression resulted in loss of the AZ surrounding ookinetes in susceptible (A) and refractory (B) mosquitoes, which survived and reached the basal lamina (bl). Note the triple membrane arrangement indicating the ookinetes are extracellular (detail boxes). Normal organelle-containing cytoplasm of the basal labyrinth lies in close proximity to the parasites.

(C) The percentage of ookinetes associated with the AZ in G3 mosquitoes, and the percentage of ookinetes associated with the AZ and/or melanization in L3–5 mosquitoes, was reduced by *TEP1* knockdown compared with the *lacZ* controls, as viewed by TEM.

(D) Immunoblot showing the full-length and cleaved forms of TEP1, visible as two bands in the hemolymph of control (c) G3 and L3–5 mosquitoes. The protein is undetectable at 4 d after dsRNA-mediated knockdown of *TEP1* (kd).

(E) TEP1-independent lytic killing of an ookinete (yellow arrow, indicating hemozoin) in a *dsTEP1* knockdown refractory midgut at 48 hpi. The ookinete is completely lysed and thus visible by light microscopy, but not TEM (i). Both the ookinete and the upper live (GFP) ookinete (blue arrow) are phalloidin-negative (ii), but phalloidin stains surrounding muscle fibers red. (iii) Merged image.

Scale bars = 1 μm in main TEM pictures and 0.1 μm in TEM detail boxes; 10 μm in (E).

doi:10.1371/journal.ppat.0020133.g005

hemocoelic origin of the PPO cascade precursors [6]. Typically, melanin was deposited in the confined spaces between the AZ membrane and the ookinete in the extracellular space (Figure 2D and 3F). In some rare cases, however, a triple layer was observed, consisting of first an AZ, then a melanin, and finally a second AZ layer (not shown). The association of the AZ with melanization and dead parasites led us to suspect that AZ formation could be a refractory killing mechanism, a hypothesis also suggested by [14,17]. We therefore focused on the prevalence of AZ formation associated with dead parasites in the refractory L3–5 strain, using the more quantitative method of phalloidin staining with fluorescence microscopy.

AZ Formation and Melanization Are Linked in Refractory Mosquitoes

Figure 4 details the relative proportions of live, dead, melanized, and AZ-associated ookinetes in susceptible and refractory mosquito midguts, as determined by fluorescence and confocal microscopy. Not surprisingly, the majority (84.9%) of ookinetes in refractory L3–5 mosquitoes were already dead by 28 hpi (Figure 4B), and by 48 hpi, killing was almost total (99.5%), compared with just 13.4% at 24 hpi and 26.5% at 48 hpi in susceptible G3 mosquitoes (Figure 4A). In the G3 strain, only a small minority of parasites were surrounded by a phalloidin-stained AZ (1.8% at 24 hpi and 5.8% at 48 hpi overall). In contrast, in the L3–5 strain a phalloidin-positive AZ surrounded 41.2% and 22.3% of ookinetes at 24 hpi and 48 hpi, respectively. The relative weakness of the phalloidin staining in G3 mosquitoes meant that fewer dead parasites could be detected in association with the AZ than were observed by TEM (see Figure 2G). Melanization was absent in G3 mosquito midguts, but it was the predominant feature associated with ookinetes in L3–5 midguts (62.2% of all parasites at 28 hpi and 86.3% by 48 hpi were melanized). Furthermore, in this strain, we noted that the formation of the AZ was invariably accompanied by the appearance of melanin. These results strongly suggest that AZ formation in refractory insects is linked to, and possibly a consequence of, melanization. Of note, however, is that in the L3–5 strain, approximately one in four of all ookinetes at 28 hpi, and one in eight at 48 hpi, were dead but showed no evidence of melanization or a surrounding AZ (Figure 4B; see also Figure 3I). We next investigated whether TEP1 activity, which is important for ookinete killing [4], could be correlated with formation of the AZ. We used dsRNA knockdown of the *TEP1* gene to address this question.

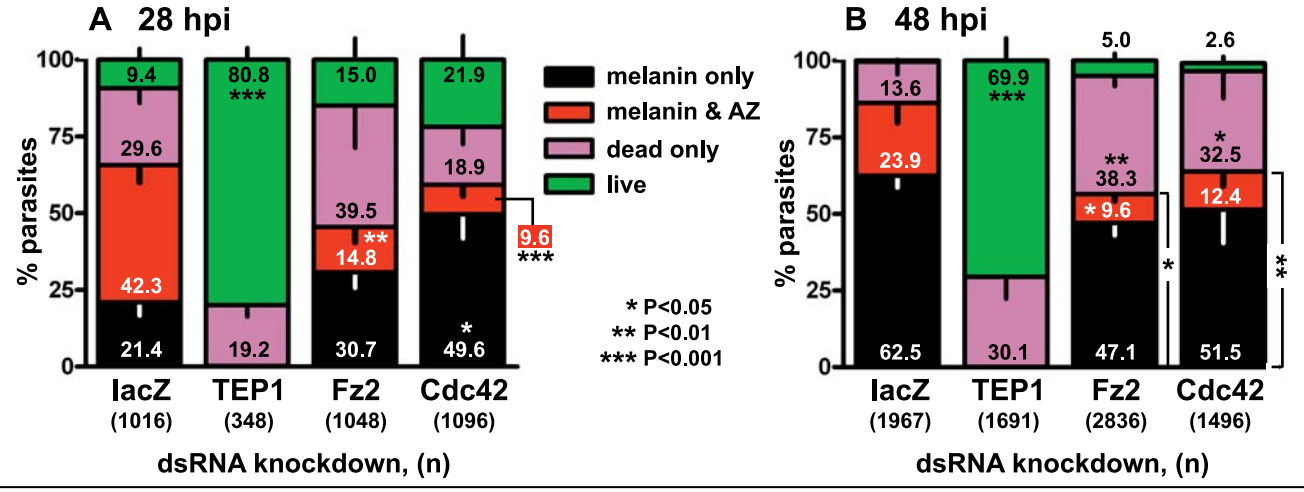

oocyst survival

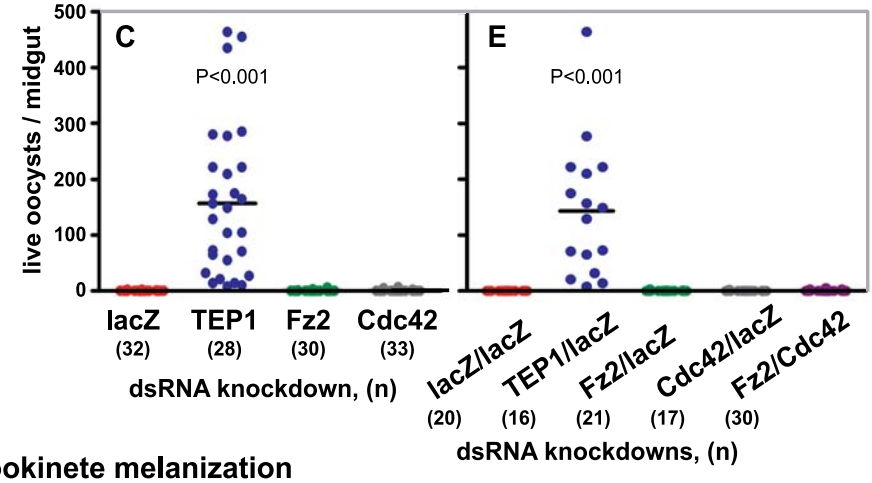

ookinete melanization

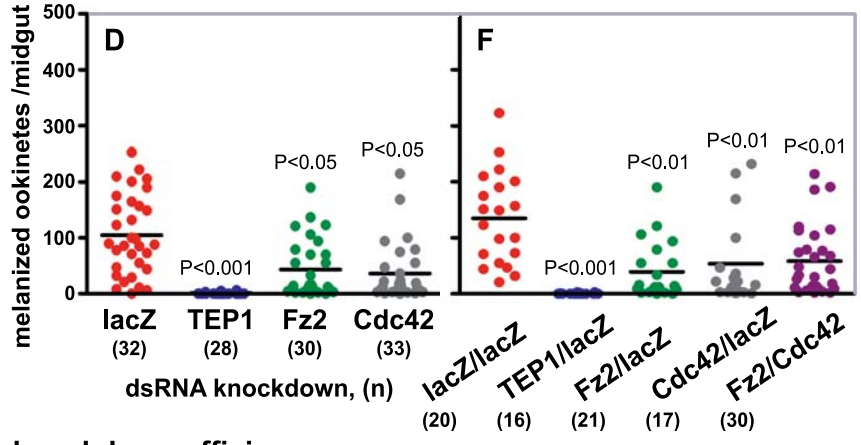

G knockdown efficiency

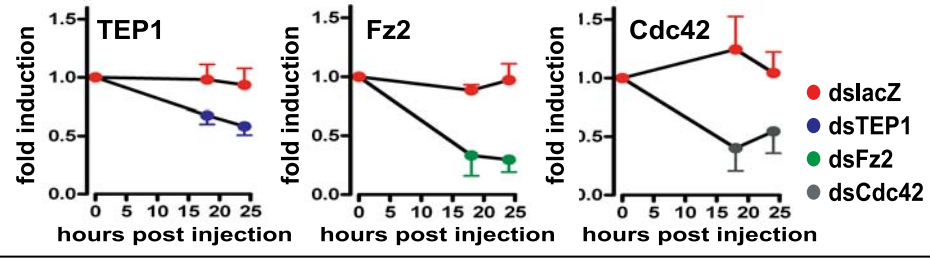

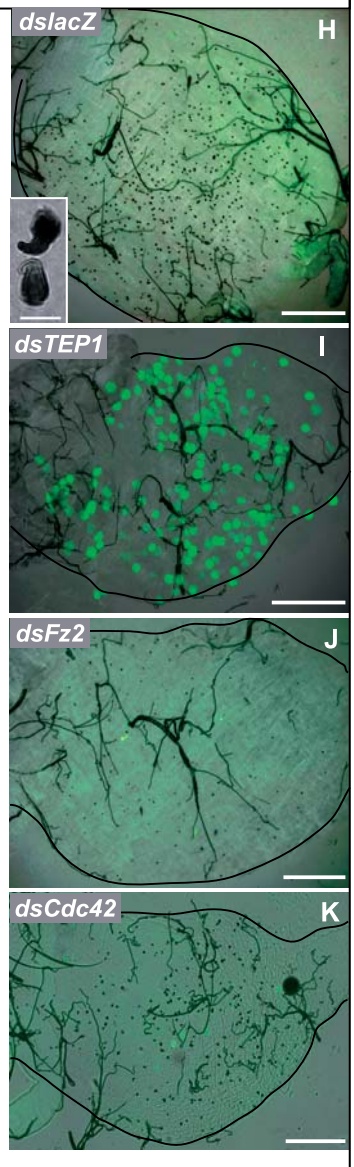

Figure 6. Knockdown of *Fz2* and *Cdc42* Disrupts AZ Formation and Melanization, but Does Not Prevent Ookinete Killing

Refractory mosquitoes were injected with *dsFz2* and *dsCdc42* and infected with *P. berghei*.

The percentage of melanized ookinetes surrounded by the AZ at (A) 28 hpi and (B) 48 hpi was reduced by injection of *dsFz2* and *dsCdc42,* compared with the *dslacZ*-injected control insects. Killing was also delayed compared with the *lacZ* controls, in which no live parasites remained by 48 hpi (B). Consequently, the number of dead parasites that exhibit neither melanization nor a surrounding AZ was increased by *Fz2* and *Cdc42* knockdown, while the total amount of melanized ookinetes was reduced. Parentheses indicate number of ookinetes counted. Mean values from three independent experiments. Bars = standard error of the mean.

Ookinete survival at 7 dpi was gauged by counting GFP oocysts. *TEP1* knockdown significantly increased parasite survival, compared with *dslacZ*-injected controls (C and H), and abolished melanization (D). *Fz2* and *Cdc42* knockdowns did not affect parasite survival (C), but did significantly diminish melanization (D). *Fz2/Cdc42* double knockdowns did not significantly improve survival (E) nor reduce melanization below the single knockdown levels (F). Combined results for four independent experiments (single knockdowns) and two experiments (double knockdowns). Bar in graphs indicates mean value; sample sizes shown in parentheses. Knockdown efficiencies (G) were assessed for each gene. The fold induction was calculated relative to the expression level of each gene before injection of dsRNA (time 0) and normalized using an internal control gene. In each case, gene expression was partially inhibited by dsRNA injection but remained unaffected by *dslacZ* treatment. Mean values ± standard error of the mean (two experiments, ten mosquitoes per group).

Photos of representative infected midguts for each knockdown phenotype, showing green fluorescent oocysts (I) and dead melanized ookinetes ([H, J, and K] and [H], inset). Note that hemozoin clusters remaining from fully lysed, non-melanized ookinetes are not visible at low magnification.

Scale bars = 200 μm (10 μm in detail box).

doi:10.1371/journal.ppat.0020133.g006

TEP1 Is Required for AZ Formation and Melanization

Knockdown of *TEP1* by dsRNA injection enables the majority of ookinetes to survive to the oocyst stage in both the G3 and L3–5 mosquito strains [4]. The efficiency of the *TEP1* knockdown by dsRNA injection was confirmed by immunoblotting of the hemolymph 4 d after injection (Figure 5).

We next studied the ultrastructure of the *TEP1* knockdown phenotype, and observed the remarkable abolition of AZ formation around ookinetes in both susceptible and refractory mosquitoes, and also the loss of ookinete melanization in the refractory strain (Figure 5A–5C). The knockdown of *TEP1* had no effect on general midgut morphology, as viewed by TEM (unpublished data). In the *TEP1* knockdown mosquitoes, we still observed dead ookinetes that had been lysed independently of TEP1. These ookinetes also failed to display any evidence of melanization or AZ formation (Figure 5E), indicating the requirement for TEP1 in these phenomena. Live, extracellular ookinetes lacking an associated AZ and melanin were frequently observed at the basal lamina in both strains, lying in close proximity to the normal organelle-containing cytoplasm of the epithelial cell basal labyrinth. The above results show that TEP1 activity is required for AZ formation and ookinete melanization in addition to being required for ookinete killing. Two hypotheses can explain these observations. First, TEP1 could control ookinete killing directly by activating AZ formation and melanization. Alternatively, melanization and AZ formation might be triggered later by the death of parasites killed by TEP1-dependent mechanisms. Therefore, to determine whether formation of the AZ is lethal to ookinetes, we used dsRNA knockdown to disrupt actin polymerization (and thereby formation of the AZ), and gauged its effect on ookinete survival.

Knockdown of *Fz2* and *Cdc42* Reduces the Formation of the AZ and Melanization

To disrupt actin polymerization, we selected to knock down the genes *Fz2* and *Cdc42,* which both control cytoskeletal rearrangements. The aim was to impair AZ formation whilst keeping the activity of TEP1 intact, and thereby examine the functional role of the AZ in ookinete killing. In a parallel microarray study by our group, we identified *Fz2* as a gene up-regulated with *TEP1* in *P. berghei*–infected *A. gambiae* midguts (S. Wyder, P. Irving, S. H. Shiao, L. Troxler et al., unpublished data). Whole-body *Fz2* expression is also induced by a non-infectious blood meal in *A. gambiae* (*A. gambiae* Gene Expression Profile, http://www.angaged.bio.uci.edu). *Fz2* encodes a seven-pass transmembrane receptor protein with described roles in *Drosophila* development, namely in establishing epithelial cell polarity during embryogenesis (reviewed by [27]). We also chose to study the Rho family guanosine triphosphate–binding cytoplasmic protein Cdc42, primarily for its published roles in actin polymerization and filopodium formation in other animals (e.g., [28]). *Cdc42* was not regulated in our microarray analysis and shows only a minor up-regulation after a non-infectious blood meal (http://www.angaged.bio.uci.edu). The roles of these genes in adult insects are, however, not well defined.

Our studies focused on refractory L3–5 strain mosquitoes in which we could observe prominent phalloidin staining for polymerized filamentous actin under fluorescence microscopy. The effects of AZ disruption were first investigated at early time-points (28 and 48 hpi) to correspond with the peak times of ookinete killing and appearance of melanin and the AZ. We performed dsRNA knockdown of the *Fz2* and *Cdc42* genes 4 d prior to *P. berghei* infection and made differential counts in L3–5 mosquito midguts of the following: (i) ookinetes positive for green fluorescent protein (GFP) (live), (ii) ookinetes surrounded by a phalloidin signal (polymerized actin), (iii) ookinetes surrounded by melanin (dead), and (iv) unstained ookinetes (dead but not melanized). The efficiency of *TEP1, Fz2,* and *Cdc42* knockdown by dsRNA was confirmed by quantitative real-time PCR analysis at 18 and 24 hours post-injection. Corresponding gene induction was reduced to 0.58, 0.30, and 0.40 times the pre-injection level, respectively, while the control, *dslacZ,* had little effect (see Figure 6).

Fz2 or *Cdc42* knockdown did not have significant effects on the normal mosquito midgut morphology, as examined by TEM (an example is given in Figure 7F). This shows that the cell-polarizing developmental phenotype of *Fz2* is not disrupted by RNAi in adult midgut cells. There was also no unusual die-off of infected *dsFz* or *dsCdc42* knockdown mosquitoes compared with the *dslacZ* controls (unpublished data).

Knockdown of *Fz2* or *Cdc42* resulted in both a significant decrease in the percentage of parasites surrounded by phalloidin-positive material, and a corresponding increase in the percentage of surviving ookinetes at 28 hpi and 48 hpi compared with the *dslacZ* control mosquitoes (Figure 6A and

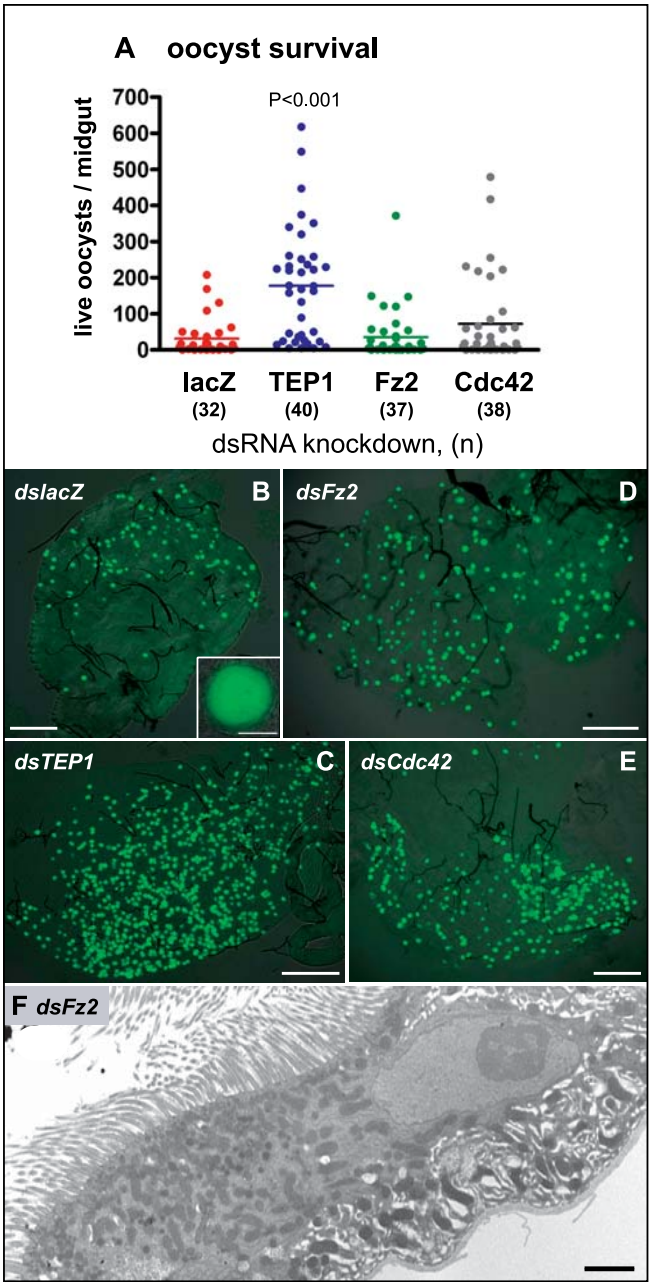

Figure 7. RNAi of *Fz2* and *Cdc42* Does Not Prevent Killing of Ookinetes in Susceptible (G3) Mosquitoes

Mosquitoes were injected with dsRNA and infected with *P. berghei*, and parasite survival at 7 dpi was gauged by counting live GFP-expressing oocysts (A). *TEP1* knockdown significantly increased parasite survival compared with *dslacZ*-injected controls (A–C). *DsFz2* and *dsCdc42* knockdowns did not significantly affect parasite survival (A, D, and E). Included are photos of representative infected midguts for each phenotype (B–E), showing GFP-expressing oocysts ([B], inset). Combined results for four independent experiments are shown. Bar in graphs indicates mean value; sample sizes shown in parentheses. (F) Midguts from *dsFz2* (shown) and *dsCdc42* (not shown) knockdown G3 mosquitoes appear to have normal morphology, as shown by TEM.
Scale bars = (B–E), 200 μm (10 μm in detail box); (F), 1 μm.
doi:10.1371/journal.ppat.0020133.g007

6B). The *Fz2* knockdown mosquitoes also contained a lower percentage of melanized parasites overall, and at 48 hpi both *Fz2* and *Cdc42* knockdown mosquitoes had significantly fewer melanized parasites (of which even fewer were associated with phalloidin staining) than the controls. In addition, we observed that melanization of ookinetes was often aberrant or incomplete in the *Fz2* and *Cdc42* knockdown mosquitoes, resulting in semi-transparent capsules or thin crescents of melanin limited to a small area of the parasite surface (not shown).

These results indicated that *Fz2* and *Cdc42* are important for the assembly of the AZ and (by an unknown relationship) for melanization. We therefore next investigated whether perturbation of these events by the knockdown of *Fz2* and *Cdc42* would result in increased numbers of surviving oocysts.

Interfering with AZ Formation and Melanization Does Not Affect Ookinete Survival

We gauged ookinete survival in *dsCdc42* and *dsFz2* knockdown L3–5 mosquitoes at 7 days post-infection (dpi) by counting the total numbers of GFP-expressing oocysts per midgut. Melanized (dead) ookinetes were also quantified at this time-point.

The important result of this experiment is that the knockdown of either *Fz2* or *Cdc42* did not ultimately lead to a significant increase in ookinete survival in refractory mosquitoes, compared with the control *dslacZ*-injected mosquitoes (Figure 6C and 6D).

In the L3–5 strain, where ookinete killing is virtually 100%, significantly fewer ookinetes were melanized in the *Fz2* and *Cdc42* knockdown mosquito midguts compared with the *lacZ* controls (melanization was reduced by 47% and 66%, respectively), indicating that although Fz2 and Cdc42 are important for the mosquito melanization response to parasites, killing can still occur even when melanization is suppressed.

The individual knockdown phenotypes for *Fz2* and *Cdc42* were remarkably similar, suggesting that these molecules could be part of the same functional process. We next examined whether these phenotypes would be exacerbated in double knockdowns (Figure 6E and 6F). The double knockdown of *Fz2/Cdc42* did not result in a significant increase in live oocysts, nor in a reduction in melanized ookinetes, compared with the single knockdowns. This could be interpreted as *Fz2* and *Cdc42* belonging to the same pathway, but it is also possible that the knockdowns were not sufficiently complete to allow us to detect a difference.

Finally, we tested the effects of *Fz2* and *Cdc42* dsRNA knockdown on ookinete survival at 7 dpi in susceptible mosquitoes. Once again, ookinete survival was not significantly increased by knockdown of either *Fz2* or *Cdc42* compared with that of the control *dslacZ*-injected mosquitoes (Figure 7).

The essential result is that the processes of AZ formation and melanization are both partially disrupted by the knockdown of *Cdc42* and *Fz2*. However, this disruption does not translate into improved ookinete survival.

Discussion

In this study we examined the ultrastructure of *P. berghei* ookinete invasion of the *A. gambiae* midgut, and possible mechanisms of *P. berghei* killing by refractory mosquitoes. Our TEM microscope studies consistently demonstrated that the ookinetes are predominantly located in the extracellular space, where they are exposed to hemocyte-derived soluble

immunity factors, rather than in intracellular locations. We hypothesize that intracellular invasion is minimized to a very transient phase, and is localized to the most apical part of a single midgut cell at the microvillous (luminal) side of the epithelium and close to the cell junction. Thereafter, the ookinete rapidly exits the cell from the basal side, or moves laterally towards the basal lamina through the narrow intercellular space. Ookinetes finally reside in an extracellular space of the membranous labyrinth, next to the basal lamina. Significantly, dead ookinetes are found consistently in this compartment, and we conclude that the major site of ookinete killing is the extracellular space, where killing is mediated by hemocyte-derived soluble factors. The dead ookinetes are surrounded by a zone of polymerized actin (the AZ), which is formed in adjacent host epithelial cells. We used a combination of confocal fluorescent microscopy and TEM with RNAi technology to demonstrate that formation of the AZ structure is triggered specifically by the presence of a *P. berghei* ookinete (a dead one in refractory mosquitoes) at the basal side of the midgut, and in the absence of apparent epithelial damage, as judged by TEM.

We further demonstrated that formation of the AZ is dependent on *TEP1, Fz2,* and *Cdc42*. We were interested in the possibility that formation of the AZ could be an ookinete killing mechanism in refractory mosquitoes. However, RNAi knockdown experiments, where we partially abolished the AZ and melanization, clearly established that in contrast to TEP1, Fz2 and Cdc42 do not induce killing of parasites. Our results separate the mechanisms of parasite killing from subsequent reactions manifested by AZ formation and melanization.

We propose that, in response to *Plasmodium* infection, the mosquito mounts a form of wound-healing response that is directed towards a dead or dying ookinete. Classical midgut tissue repair/healing processes and AZ formation probably respond to a common basic stimulus (i.e., abnormal or damaged tissue), but in the case of AZ formation, it is a moribund parasite that provides this signal. The AZ reaction is characterized by actin polymerization and PPO activation, which is characterized by melanization in refractory mosquitoes.

We have now identified a component of the AZ as polymerized actin and shown that the presence of the AZ and melanin is a predominant feature associated with dead ookinetes in refractory mosquitoes. In our *A. gambiae–P. berghei* infection model, the AZ is morphologically distinct from other zones of polymerized actin that occur throughout the midgut, which assist the expulsion of dead epithelial cells and repair the remaining tissue [15–18]. In contrast to this tissue repair process, the AZ is specifically provoked in the presence of a parasite, is only formed by the most basal part of the midgut cell, does not appear to facilitate cell expulsion, and is linked in an unknown way to melanization in refractory mosquitoes. All the midgut cells in contact with the ookinete contribute to the AZ, and all the cells appear to be healthy. Apoptosis and the extrusion of infected cells was also minimal in our study, suggesting that intracellular modes of ookinete killing are less prevalent in *A. gambiae* infected with *P. berghei* than in *A. stephensi* infected with *P. berghei* [15,16,21–25]. However, it would be inappropriate to make direct comparisons between analyses involving different host–parasite species combinations. In our study, ookinetes did not undergo phagocytosis in the midgut. Midgut cells are non-phagocytic; furthermore, our TEM observations of ookinete phagocytosis by cultured mosquito cells in vitro were very distinct structurally from anything seen by us in the midgut (S. Shiao, unpublished data).

In our study, dsRNA knockdown of *Cdc42* and *Fz2* decreased AZ formation in refractory mosquitoes. Unexpectedly, melanization was also impaired, in terms of both intensity and the total number of melanized parasites. This strongly suggests a link between the AZ and melanization. The exact relationship between the AZ and melanization is complex and may also involve other factors, because a thinner AZ can form around a small percentage of non-melanized ookinetes in susceptible mosquitoes. In some arthropods the upstream phenoloxidase component of the melanization cascade can aid wound healing by cross-linking clot fibers, possibly via transglutaminase activity [20,29,30]. Should this reaction occur in G3 mosquitoes, it would not result in easily detectable melanin, which is in contrast to the L3–5 strain, where production of melanin is overtly exaggerated and demonstrable with the tools used in our study. It would be interesting in this respect to determine whether, in susceptible G3 strain mosquitoes, the strength of AZ formation could be increased by the knockdowns of *C-type lectin 4, SRPN2,* or *SRPN6,* which lead to massive spontaneous melanization reactions [5,12,31]. Furthermore, these knockdowns and double knockdowns of *Fz2*/*SRPN6* and *Cdc42*/*SRPN6* in L3–5 mosquitoes would provide more insight into the importance of melanization in AZ formation.

The role of Cdc42 in AZ actin polymerization in L3–5 mosquitoes was not unexpected, because in other animals this cytoplasmic Rho family guanosine triphosphate–binding protein controls a wide array of cellular processes, including filopodium formation (via activation of Wiskott-Aldrich syndrome protein, profilin, the Arp2/3 complex, and finally, actin nucleation; reviewed by [28,32,33]). To our knowledge, however, this is the first study to implicate *Fz2* in the control of actin polymerization in adult insects, and *Fz2* and *Cdc42* in the melanization response. Frizzled proteins are seven-pass transmembrane cell surface receptors that mediate the Wnt protein signaling necessary for development and establishing cell polarity in several embryonic tissues in *Drosophila,* including the midgut epithelium and the developing primordium of the adult wing (e.g., [27,34–36]). Many of these processes require coordination or remodeling of the cytoskeleton, especially at the apical side of polarized cells.

The double knockdown of *Fz2/Cdc42* did not significantly alter the single knockdown phenotype, implying that both molecules could be part of the same biochemical process, possibly with Fz2 acting as a transmembrane receptor upstream of the cytoplasmic Cdc42. Alternatively, the knockdowns were not sufficiently complete to allow us to detect a difference in the phenotype. The current data do not allow us to distinguish between these two possibilities. Clearly, the parasites did not utilize host actin polymerization or Cdc42 activities to achieve intracellular invasion, a mode of invasion recruited by certain bacteria (e.g., *Shigella* and *Listeria* [37–39]). The AZ was never associated with intracellular ookinetes, and we did not see unusually greater numbers of intracellular parasites in *Cdc42* or *Fz2* knockdown midguts (unpublished data).

We do not exclude at this stage an alternative role of Fz2 and Cdc42 in controlling hemocyte cytoskeletal rearrange-

ments that allow secretion of defense factors including TEP1, PPO, or leucine-rich repeat immune protein 1. We are currently investigating whether this could account for the transiently improved survival of ookinetes between 24 and 48 hpi in the *Fz2* and *Cdc42* knockdown mosquitoes.

Materials and Methods

TEM. TEM ultrastructural studies were conducted to analyze (i) *P. berghei* invasion and compartmentalization, (ii) formation of the AZ and melanization in control and dsRNA knockdown mosquitoes, and (iii) the morphology of *Fz2* and *Cdc42* knockdown midguts.

Midguts were dissected in 0.1 M phosphate buffer at 18, 21, 22, 23, 24, 28, 33, 44, and 48 hpi, and fixed with 4% glutaraldehyde. Samples were post-fixed in 1% osmium tetroxide, rinsed, dehydrated through a graded ethanol series, and embedded in araldite resin. A series of semi-thin sections were screened by toluidine blue staining, and several ultra-thin sections per sample were transferred to copper grids and stained with uranyl acetate and lead citrate. Sections were observed at 60 kV on a Hitachi (http://www.hitachi.com) 7500 transmission electron microscope.

In total, 137 individual ookinetes in G3 mosquitoes and 93 in L3–5 mosquitoes were screened by TEM.

dsRNA injection and mosquito infections. An *Fz2* Xho1-EcoR1 450-bp-long fragment and a *Cdc42* Xho1-Sma1 500-bp-long fragment were cloned from the Gateway system library (Invitrogen, http://www.invitrogen.com) clones 33DG01 (ENSANGT00000023104) and 20AD06 (ENSANGT00000022573), respectively, into the pLL10 vector. Plasmids pLL10, pLL17 *(dsTEP1),* and pLL100 *(dslacZ),* and the synthesis of dsRNAs, were constructed as previously described [4,40].

A. gambiae–susceptible G3 and refractory L3–5 strains were maintained at 28 °C, 75%–80% humidity, and a 12/12 h light/dark cycle. Female 2-d-emerged adult mosquitoes from the same cohort were injected with 0.2 μg of dsRNA using a Nanoject II injector (Drummond, http://www.drummondsci.com). Co-injection experiments were performed by injecting a double volume of 1:1 mixtures of 3-μg/μl solutions of dsRNAs.

Mosquitoes were infected 4 d after dsRNA injection. In each infection experiment, mosquitoes were fed on an anesthetized ICR mouse that had been infected with *P. berghei* GFP_{CON} 259cl2 clone 16 [41]. The parasitemia in mice was assessed using Diff-Quik I (Dade Behring, http://www.dadebehring.com)–stained blood smears for the proportion of infected red blood cells and differentiated gametocytes, and gametocytemia was established by FACS analyses of 10,000 infected red blood cells.

RNAi efficiency was assessed by quantitative real-time PCR. Total RNA from ten mosquitoes was extracted with Trizol reagent (Invitrogen) before and after injection of dsRNA, and reverse transcribed using M-MLV enzyme with random primers (Invitrogen). Specific primers were designed using PrimerSelect (DNAStar, http://www.dnastar.com): for *Cdc42,* forward 5′-CGCCGTCACGGTCATGA-3′, reverse 5′-CTGGCCAGCTGTGTCAAACA-3′; for *Fz2,* forward 5′-GAATCGAGATCGACTGCCTTTAA-3′, reverse 5′-GTAATGCTTCTCTCTTGCTCTCGTT-3′; for *TEP1,* forward 5′-ATACGGATCTCAGCTACACCAAATC-3′, reverse 5′-GCTTGCGGGCCTTGAT-3′; and for *Ribosomal protein L19* (internal control gene), forward 5′- CCAACTCGCGACAAAACATTC-3′, reverse 5′- ACCGGCTTCTTGATGATCAGA-3′. The reactions were run on an Applied Biosystems 7500 Fast Real-Time PCR System using Power SYBR Green Mastermix (http://www.appliedbiosystems.com).

Fluorescence microscopy. Mosquito midguts were dissected at 28, 32, and 48 hpi, corresponding to critical stages during ookinete traversal of the midgut and ookinete killing, and between 7 and 10 dpi to determine the abundance of surviving GFP-expressing oocysts. Midguts were dissected and washed on ice, fixed in 4% paraformaldehyde at room temperature for 30 min, then washed with phosphate buffered saline. To visualize polymerized filamentous actin, fixed midguts were incubated with rhodamine-conjugated phalloidin (Molecular Probes, http://probes.invitrogen.com) for 1 h, washed in phosphate buffered saline, and counterstained with DAPI and mounted with Vectashield (Vector Labs, http://www.vectorlabs.com). β-tubulin was stained with Cy5-conjugated paclitaxel (Taxol; Molecular Probes), and non-polymerized (globular) α-actin with monoclonal anti-α-actin antibody (Sigma, http://www.sigmaaldrich.com). Dead parasites were detected with polyclonal antibody against TEP1 [4].

Ookinete and oocyst numbers were scored using a Zeiss fluorescence microscope (Axiovert 200M) equipped with a Zeiss Apotome module (http://www.zeiss.com). Live parasites were identified by GFP fluorescence, whereas dead non-fluorescent parasites were identified by characteristic dense hemozoin clusters in the absence of an enclosing cell membrane (described in [14]), or by melanization. These experiments were repeated at least four times. Differential ookinete staining percentages were calculated at 28 hpi and 48 hpi from the mean of three random fields of view per midgut under 63× magnification. Three independent experiments were conducted, each with 12 to 23 midguts per treatment group. Images were reconstructed and analyzed using Axiovision 4.37 software (Zeiss) and UTHSCSA Image Tool 3 (http://ddsdx.uthscsa.edu/dig/itdesc.html), and all parasite counts were statistically compared using one-way ANOVA with Bonferroni's post-test (GraphPad Prism 3; GraphPad Software, http://www.graphpad.com).

For confocal microscopy, fixed midguts were prepared as above and analyzed with a Zeiss LSM 510 confocal microscope. Images were processed with the Zeiss LSM 510 Image Browser.

Candidate gene selection by microarray analysis. Briefly, midguts taken at 24 and 48 hpi from *P. berghei*-infected transgenic TEP1 gain-of-function (7a), wild-type (G3), and TEP1 loss-of-function (7b) *A. gambiae* mosquitoes were subjected to Affymetrix chip microarray analysis (http://www.affymetrix.com). Arrays were screened for TEP1-coregulated candidate genes (7a > G3 > 7b by a factor of at least 2-fold at 24 hpi) using the dCHIP filter analysis (Genespring; Agilent Technologies, http://www.agilent.com).

Acknowledgments

The authors thank Valérie Demais for assistance with the electron microscope platform at the Institut Fédératif de Recherche de Neurosciences de Strasbourg, and Jerome Mutterer for access to the confocal microscopy facility platform at the Institut de Biologie Moléculaire des Plantes, Strasbourg. Stefan Wyder and Phil Irving are gratefully acknowledged for performing microarray analyses at the Institut de Biologie Moléculaire et Cellulaire. GFP_{CON} parasites were kindly donated by Dr. A. P. Waters, LUMC, Leiden, The Netherlands. For special training, S.-H. S. and M. M. A. W. wish to thank the organizers of the EMBO/EU Practical Course on Electron Microscopy.

Author contributions. SHS and EAL conceived and designed the experiments. SHS and MMAW performed the experiments. SHS, MMAW, and DZ analyzed the data. DZ and EAL contributed reagents/materials/analysis tools. MMAW, JAH, and EAL wrote the paper.

Funding. This work was financially supported by the Centre National de la Recherche Scientifique (UPR 9022), the Institut National de la Recherche Medicale (INSERM "Avenir" to EAL), the Fondation Schlumberger (FSER fellowships to EAL, SHS, and MMAW) and the European Commission FP6 (Networks of Excellence "BioMalPar" to EAL and JAH). EAL is an International Research Scholar of the Howard Hughes Medical Institute.

Competing interests. The authors have declared that no competing interests exist.

References

1. Levashina E (2004) Immune responses in *Anopheles gambiae*. Insect Biochem Mol Biol 34: 673–678.
2. Michel K, Kafatos FC (2005) Mosquito immunity against *Plasmodium*. Insect Biochem Mol Biol 35: 677–689.
3. Holt RA, Subramanian GM, Halpern A, Sutton GG, Charlab R, et al. (2002) The genome sequence of the malaria mosquito *Anopheles gambiae*. Science 298: 129–149.
4. Blandin S, Shiao SH, Moita LF, Janse CJ, Waters AP, et al. (2004) Complement-like protein TEP1 is a determinant of vectorial capacity in the malaria vector *Anopheles gambiae*. Cell 116: 661–670.
5. Osta MA, Christophides GK, Kafatos FC (2004) Effects of mosquito genes on *Plasmodium* development. Science 303: 2030–2032.
6. Paskewitz SM, Brown MR, Lea AO, Collins FH (1988) Ultrastructure of the encapsulation of *Plasmodium cynomolgi* (B strain) on the midgut of a refractory strain of *Anopheles gambiae*. J Parasitol 74: 432–439.
7. Christensen BM, Li J, Chen CC, Nappi AJ (2005) Melanization immune responses in mosquito vectors. Trends Parasitol 21: 192–199.
8. Zheng L, Wang S, Romans P, Zhao H, Luna C, et al. (2003) Quantitative trait loci in *Anopheles gambiae* controlling the encapsulation response against *Plasmodium cynomolgi* Ceylon. BMC Genet 4: 16.
9. Sinden RE, Alavi Y, Raine JD (2004) Mosquito–malaria interactions: A

reappraisal of the concepts of susceptibility and refractoriness. Insect Biochem Mol Biol 34: 625–629.
10. Collins FH, Sakai RK, Vernick KD, Paskewitz S, Seeley DC, et al. (1986) Genetic selection of a *Plasmodium*-refractory strain of the malaria vector *Anopheles gambiae*. Science 234: 607–610.
11. Whitten MMA, Shiao SH, Levashina EA (2006) Mosquito midguts and malaria: Cell biology, compartmentalization and immunology. Parasite Immunol 28: 121–130.
12. Abraham EG, Pinto SB, Ghosh A, Vanlandingham DL, Budd A, et al. (2005) An immune-responsive serpin, SRPN6, mediates mosquito defense against malaria parasites. Proc Natl Acad Sci U S A 102: 16327–16332.
13. Vlachou D, Schlegelmilch T, Christophides GK, Kafatos FC (2005) Functional genomic analysis of midgut epithelial responses in *Anopheles* during *Plasmodium* invasion. Curr Biol 15: 1185–1195.
14. Vernick KD, Fujioka H, Seeley DC, Tandler B, Aikawa M, et al. (1995) *Plasmodium gallinaceum:* A refractory mechanism of ookinete killing in the mosquito, *Anopheles gambiae*. Exp Parasitol 80: 583–595.
15. Han YS, Thompson J, Kafatos FC, Barillas-Mury C (2000) Molecular interactions between *Anopheles stephensi* midgut cells and *Plasmodium berghei:* The time bomb theory of ookinete invasion of mosquitoes. EMBO J 19: 6030–6040.
16. Han YS, Barillas-Mury C (2002) Implications of Time Bomb model of ookinete invasion of midgut cells. Insect Biochem Mol Biol 32: 1311–1316.
17. Vlachou D, Zimmermann T, Cantera R, Janse CJ, Waters AP, et al. (2004) Real-time, in vivo analysis of malaria ookinete locomotion and mosquito midgut invasion. Cell Microbiol 6: 671–685.
18. Gupta L, Kumar S, Han YS, Pimenta PFP, Barillas-Mury C (2005) Midgut epithelial responses of different mosquito-*Plasmodium* combinations: The actin cone zipper repair mechanism in *Aedes aegypti*. Proc Natl Acad Sci U S A 102: 4010–4015.
19. Benink HA, Bement WM (2005) Concentric zones of active RhoA and Cdc42 around single cell wounds. J Cell Biol 168: 429–439.
20. Bidla G, Lindgren M, Theopold U, Dushay MS (2005) Hemolymph coagulation and phenoloxidase in *Drosophila* larvae. Dev Comp Immunol 29: 669–679.
21. Baton LA, Ranford-Cartwright LC (2004) *Plasmodium falciparum* ookinete invasion of the midgut epithelium of *Anopheles stephensi* is consistent with the Time Bomb model. Parasitol 129: 663–676.
22. Herrera-Ortiz A, Lanz-Mendoza H, Martinez-Barnetche J, Hernandez-Martinez S, Villarreal-Trevino C, et al. (2004) *Plasmodium berghei* ookinetes induce nitric oxide production in *Anopheles pseudopunctipenni*s midguts cultured in vitro. Insect Biochem Mol Biol 34: 893–901.
23. Kumar S, Gupta L, Han YS, Barillas-Mury C (2004) Inducible peroxidases mediate nitration of *Anopheles* midgut cells undergoing apoptosis in response to *Plasmodium* invasion. J Biol Chem 279: 53475–53482.
24. Danielli A, Barillas-Mury C, Kumar S, Kafatos FC, Loukeris TG (2005) Overexpression and altered nucleocytoplasmic distribution of *Anopheles* ovalbumin-like SRPN10 serpins in *Plasmodium*-infected midgut cells. Cell Microbiol 7: 181–190.
25. Kumar S, Barillas-Mury C (2005) Ookinete-induced midgut peroxidases detonate the time bomb in anopheline mosquitoes. Insect Biochem Mol Biol 35: 721–727.
26. Vanderberg JP, Yoeli M (1966) Effects of temperature on sporogonic development of *Plasmodium berghei*. J Parasitol 52: 559–564.
27. Wang HY, Liu T, Malbon CC (2006) Structure-function analysis of Frizzleds. Cell Signal 18: 934–941.
28. Cerione RA (2004) Cdc42: New roads to travel. Trends Cell Biol 14: 127–132.
29. Osaki T, Kawabata S (2004) Structure and function of coagulogen, a clottable protein in horseshoe crabs. Cell Mol Life Sci 61: 1257–1265.
30. Iijima M, Hashimoto T, Matsuda Y, Nagai T, Yamano Y, et al. (2005) Comprehensive sequence analysis of horseshoe crab cuticular proteins and their involvement in transglutaminase-dependent cross-linking. FEBS J 272: 4774–4786.
31. Michel K, Budd A, Pinto S, Gibson TJ, Kafatos FC (2005) *Anopheles gambiae* SRPN2 facilitates midgut invasion by the malaria parasite *Plasmodium berghei*. EMBO J 6: 891–897.
32. Bryant PJ (1999) Filopodia: Fickle fingers of cell fate? Curr Biol 9: R655–R657.
33. Rorth P (2003) Communication by touch: Role of cellular extensions in complex animals. Cell 112: 595–598.
34. Vinson CR, Conover S, Adler PN (1989) A *Drosophila* tissue polarity locus encodes a protein containing seven potential transmembrane domains. Nature 338: 263–264.
35. Chen C, Struhl G (1999) Wingless transduction by the Frizzled and Frizzled2 proteins of *Drosophila*. Development 126: 5441–5452.
36. Adler PN (2002) Planar signaling and morphogenesis in *Drosophila*. Dev Cell 2: 525–535.
37. Mounier J, Laurent V, Hall A, Fort P, Carlier MF, et al. (1999) Rho family GTPases control entry of *Shigella flexneri* into epithelial cells but not intracellular motility. J Cell Sci 112: 2069–2080.
38. Shibata T, Takeshima F, Chen F, Alt FW, Snapper SB (2002) Cdc42 facilitates invasion but not the actin-based motility of *Shigella*. Curr Biol 12: 341–345.
39. Cossart P, Sansonetti PJ (2004) Bacterial invasion: The paradigms of enteroinvasive pathogens. Science 304: 242–248.
40. Blandin S, Moita LF, Kocher T, Wilm M, Kafatos FC, et al. (2002) Reverse genetics in the mosquito *Anopheles gambiae:* Targeted disruption of the Defensin gene. EMBO Rep 3: 852–856.
41. Franke-Fayard B, Trueman H, Ramesar J, Mendoza J, van der Keur M, et al. (2004) A *Plasmodium berghei* reference line that constitutively expresses GFP at a high level throughout the complete life cycle. Mol Biochem Parasitol 137: 23–33.